RHO MESON PHOTOPRODUCTION FROM COMPLEX NUCLEI*

D. W. G. S. Leith

Stanford Linear Accelerator Center
Stanford University, Stanford, California 94305

(Invited talk presented at Third International Conference on
High Energy Physics and Nuclear Structure, Columbia
University, September 1969)

RHO MESON PHOTOPRODUCTION FROM COMPLEX NUCLEI*

D. W. G. S. Leith

Stanford Linear Accelerator Center
Stanford University, Stanford, California 94305

I. Introduction

Although the title refers only to photoproduction of rho mesons on complex nuclei, I wish to talk on a rather broader footing. I do this with the justification that in the spirit of the vector dominance model, (VDM), all photo-processes involve the coupling of the photon to the vector mesons. To this end I would like to review the situation on ρ^0 photoproduction on complex nuclei, the total photoabsorption cross section determinations, and the implications of these results for VDM. Finally, I will summarize the experimental results of the searches for heavy vector mesons.

Before going on to talk of photons, let us take a few minutes to review why we use nuclear targets. There are two phenomena — familiar to all of you — which lead us to use complex nuclear targets in high energy physics — diffraction and absorption. The diffraction phenomena,[1] or coherent production from each of the individual nucleons within the nucleus provides a filter for the isolation of reactions involving no change in quantum numbers (i.e., isospin, G-parity and spin-parity series remain unchanged). Such processes may then be studied preferentially to reactions involving meson exchange, spin flip, I-spin exchange, etc. A process may be coherent, and also be inelastic, (in the sense that the incoming and outgoing particles do not have the same mass), if the longitudinal momentum transfer required to make up the mass difference is small compared to the momentum required to break up the nucleus. A list of reactions which could proceed coherently on nuclear targets is given below, and includes examples involving mass changes and also excitation of the spin-parity series:

(a) Elastic scattering, in the forward direction.

(b) $p \to P_{11}$, where P_{11} is the N*(1400), a $J^P = 1/2^+$ nucleon isobar.

(c) $\pi \rightarrow A_1$, where A_1 is a 3π mesonic state of mass ~ 1080 MeV, with $J^P = 1^+$.

(d) $K \rightarrow K^*_{1300}$, where K^*_{1300} is a $K\pi\pi$ meson of mass ~ 1300 MeV, and with supposed $J^P = 1^+$.

(e) $\gamma \rightarrow \rho$, where ρ is the 750 MeV dipion resonance with $J^P = 1^-$.

The second phenomena – the absorption of the outgoing particles –, allows us the possibility of determining their attenuation in nuclear matter. If the outgoing particles live long enough to traverse the nucleus, then by varying the path length in nuclear matter (which we do by varying the size of the nucleus) and observing the relative yield, we can deduce the total cross section. Since we have a whole menagerie of unstable particles in high energy physics and no other way to measure many of their properties such as the total cross section, this is a useful technique bridging high energy physics and nuclear physics. The idea was originally used by Drell and Trefil[2] to show that the total cross section for protons on protons, derived from an experiment measuring p-A scattering,[3] was in good agreement with observed pp data. The technique is currently being used to determine the A_1-p [4] and K^*_{1300}-p [5] total cross sections, in addition to the experiments to be discussed below on the absorption of rho mesons by nucleons.

These attenuation investigations were assumed to be independent of the details of nuclear models, or indeed the details of interaction within the nucleus. It was hoped to treat the nucleus as a black box which was our variable thickness absorber in a classical experiment to measure the total cross section by attenuation. The nuclear physicists present will not be surprised to find that our naive assumptions were indeed naive! I will discuss briefly how serious these assumptions are as we come to specific issues later.

The question of studying photon interactions essentially boils down to the testing of vector dominance theory – this model has been described fully before.[6] Basically, the electromagnetic interaction of hadrons is described by the coupling of the electromagnetic field to the hadronic electromagnetic current –

$$ j_\mu^{em}(x) = j_\mu^I(x) + \frac{1}{2} j_\mu^Y(x) \quad , \tag{1} $$

where $j_\mu^I(x)$ and $j_\mu^Y(x)$ are the zero components of the isospin current and the hypercharge current respectively. The smallness of the coupling constant, $\alpha = e^2/4\pi$, allows one in most cases to treat photoproduction in lowest order of the electromagnetic interactions.

The vector dominance model then connects the hadronic electromagnetic current with the fields of the vector mesons ρ^0, ω, and ϕ which have the same quantum numbers as the electromagnetic current, namely $J = 1$, $P = -1$, $C = -1$. This connection can be made via the current field

identity —

$$j_\mu^{em}(x) = -\left[\frac{m_\rho^2}{2\gamma_\rho} \cdot \rho_\mu^o(x) + \frac{m_\omega^2}{2\gamma_\omega} \cdot \omega_\mu(x) + \frac{m_\phi^2}{2\gamma_\phi} \cdot \phi_\mu(x)\right] \equiv -\sum_V \frac{m_V^2}{2\gamma_V} \cdot V_\mu(x)$$

(2)

where γ_ρ, γ_ω, γ_ϕ are coupling constants, and m_ρ, m_ω, m_ϕ are the masses of the vector mesons.

The assumption which is being made here is that the vector mesons ρ, ω, ϕ completely satisfy this summation — or that the contribution from the three known vector mesons completely saturates the electromagnetic current. This is a very strong statement and I wish to return to it later in the talk.

According to our field-current identity, any amplitude involving real or virtual photons is a linear combination of vector meson amplitudes, each multiplied by a vector meson propagator. The assumption is then made that the invariant vector meson amplitudes are slowly varying functions of the vector meson mass m_V, — i.e., any energy dependence comes from the propagators and not the coupling constants.

Historically, the vector dominance model (VDM) had its birth with the explanation of the nucleon form factor in terms of vector meson clouds,[7] but has since been generalized to explain the hadronic interactions of the photon.[6] This model may be used to relate many processes involving photons to similar processes involving the vector mesons. It is the hope that all of these relationships will be satisfied by a single value for the vector meson-photon coupling constants. We shall discuss below several experiments attempting to measure this quantity.

II. Photoproduction of Rho Mesons from Complex Nuclei

The cross section for the photoproduction of rho mesons from nuclear targets, has been measured at DESY[8,9] (2.7-4.5 BeV), at Cornell[10] (6.2 BeV), and at SLAC[11] (at 8.8 BeV). The published results show some disagreement. I wish to describe the SLAC experiment in some detail, present some new but preliminary data, and to discuss the differences between the three experiments.

The scope of the SLAC experiment is shown in Table I. The data up to 10 BeV has been obtained using a monochromatic photon beam which has been described previously.[12] The beam is obtained from two-photon annihilation in flight of 12 BeV positrons on the orbital electrons in a liquid hydrogen target. A typical energy spectrum of the beam is shown in Fig. 1(a). The data above 10 BeV are obtained using a conventional thin target bremsstrahlung beam at 10, 13, and 16 BeV. The energy spectrum at 16 GeV is shown in Fig. 1(b). The exposures were made in such a way that one is able to test for inelastic contributions as one moves away from the end point of the bremsstrahlung spectrum by comparison of the cross sections for several energy cuts (see Fig. 1(c)). This is an especially important point in the bremsstrahlung experiment.

SYSTEMATIC STUDY OF RHO MESON PHOTOPRODUCTION
USING A WIRE SPARK CHAMBER SPECTROMETER AT SLAC

TARGET	ENERGY (GeV) MONOCHROMATIC γ's			BREMSSTRAHLUNG		
	5	7	9	10	13	16
H_2	×		×	×	×	×
D_2			×	×		×
B_e	×	×	×	×		×
C	×	×	×			
Al	×	×	×			
Cu	×	×	×			
Ag			×			
Pb	×	×	×			×

Fig. 1 (a) --The energy spectrum from the monochromatic beam at 9 BeV, (b) the thin target bremsstrahlung spectrum for 16 BeV, (c) schematic representation of the photon beam energy spectra from various runs. The shaded areas show energy cuts at corresponding points on the spectra, allowing checks to be made on the possible contribution from inelastic processes. Note that the low energy cutoff of the above spectra is due to the energy acceptance of the spectrometer.

The experimental apparatus used in this experiment is shown schematically in Fig. 2. The wire spark chamber spectrometer and the on-line IBM 1800 computer system have been described in detail elsewhere.[13] The photon flux is measured, pulse-by-pulse, by a simple e^+e pair spectrometer installed in the last sweeping magnet. To calibrate the absolute photon flux, the spark chamber system was periodically used as a pair spectrometer. The properties of the system are: (a) a large mass acceptance of ~ 1000 MeV per setting, with a maximum detectable mass of ~ 3000 MeV, (b) good mass resolution, $\sim \pm 8$ MeV, (c) large decay angular acceptance, (d) momentum transfer acceptance from 0 to 0.25 $(GeV/c)^2$, with a resolution of 0.0005 $(GeV/c)^2$ for small t, increasing to 0.002 $(GeV/c)^2$ for large t.
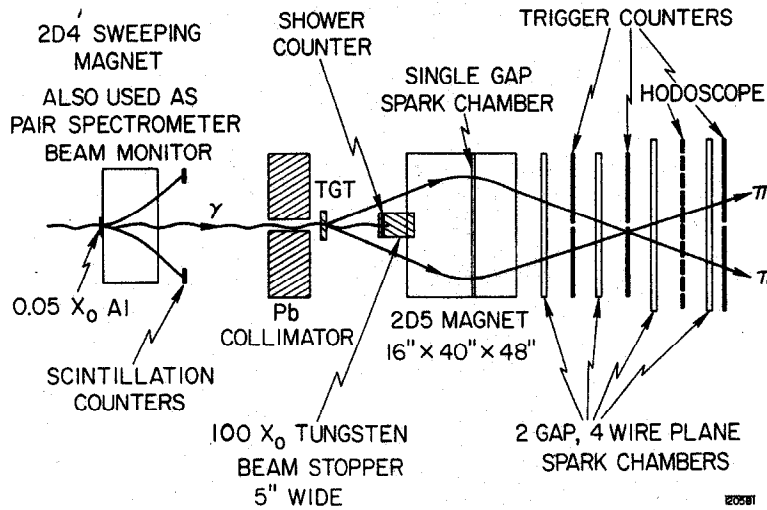

Fig. 2--The spectrometer system, showing the arrangement of the counters, the magneto-strictive read-out wire spark chambers and the two photon monitors; a pair spectrometer and a shower counter inside the tungsten beam stopper. Periodically, for calibrating the 2D4 pair spectrometer, the beam stopper was removed and the spark chamber system converted into an electron-positron pair spectrometer. For full description see Ref. 11.

The large decay angular acceptance allows us to verify that the rho mesons are indeed transversely polarized, normally an assumption in the other experiments measuring rho photoproduction. The decay distribution, evaluated in the helicity system, for rho mesons produced at 9 BeV from a Be target is shown in Fig. 3. The solid curve is the result of a fit to the distribution, evaluating the spin density matrix elements using:

$$W(\cos\theta, \phi) = \frac{3}{4\pi}\left[0.5(1-\cos^2\theta) + \rho_{00}(3/2\cos^2\theta -1/2) \right.$$
$$\left. - \rho_{1-1}\sin^2\theta\cos 2\phi - \sqrt{2}\,\mathrm{Re}\,\rho_{10}\sin 2\theta\cos\phi\right] \tag{3}$$
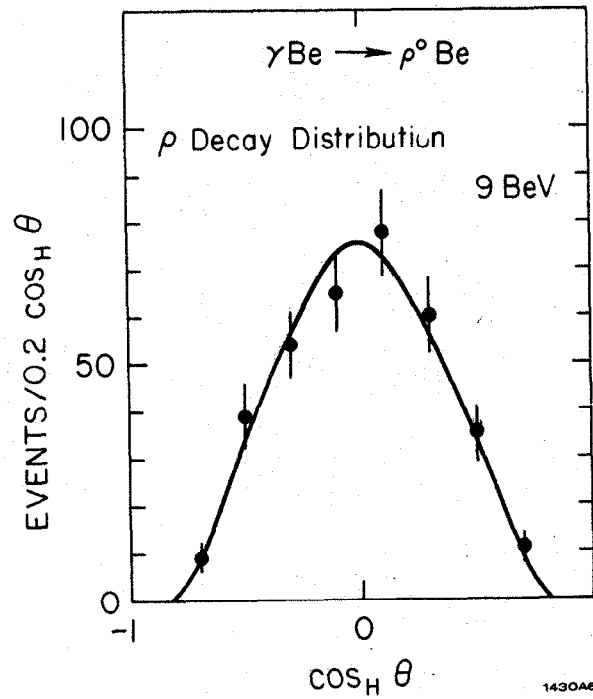
assuming

$$\rho_{00} + 2\rho_{11} = 1$$

Fig. 3--The observed decay distribution of rho mesons from Be, at 9 BeV, evaluated in the helicity system. The data includes the forward coherent peak (i.e., $t \lesssim .05 (GeV/c)^2$).
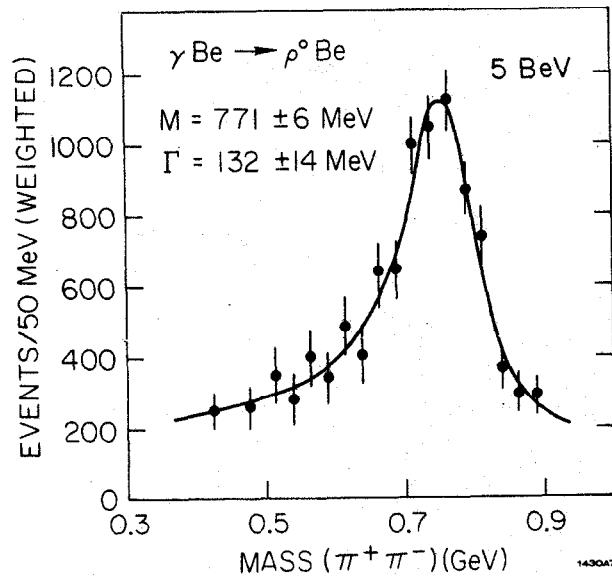

Fig. 4--The mass distribution of pion pairs produced from Be by photons from the 5 BeV monochromatic peak. The solid line is the best fit to the data using a coherent mixture of resonant and diffractive background amplitudes, as described in text.

The fit which takes into account the geometrical acceptance of the system, resulted in

$$\rho_{00} = 0.0 \pm 0.1$$

$$\rho_{1-1} = -0.03 \pm 0.05$$

$$\text{Re}\,\rho_{10} = 0.03 \pm 0.03$$

Clearly the rho mesons are produced with an essentially complete transverse alignment.

The effective mass distribution of the dipion pairs is measured for each target at each energy. Figure 4 shows the spectrum measured at 5 BeV for Be. The solid line is the result of a fit to the following model:
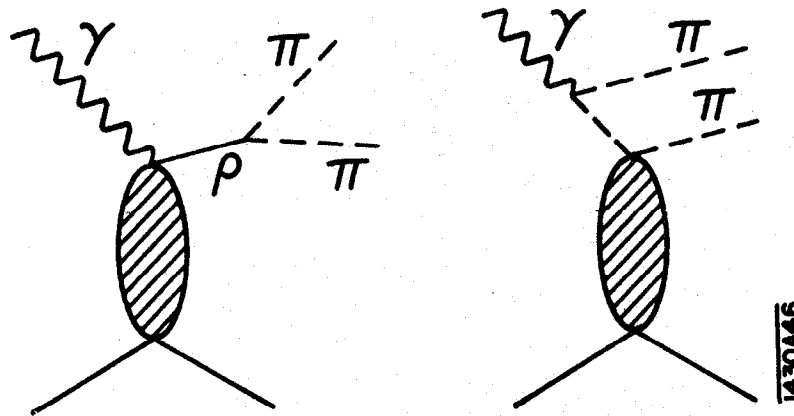
$$\frac{dN}{dM_{\pi\pi}} = C_0 M_\rho \left[\frac{M_{\pi\pi}\Gamma}{(M_\rho^2 - M_{\pi\pi}^2)^2 + M_\rho^2 \Gamma^2} + C_1 \frac{M_\rho^2 - M_{\pi\pi}^2}{(M_\rho^2 - M_{\pi\pi}^2)^2 + M_\rho^2 \Gamma^2} + C_2 \right] \quad (4)$$

where

$$\Gamma = \Gamma_\rho \frac{M_\rho}{M_{\pi\pi}} \left(\frac{M_{\pi\pi}^2 - 4\mu^2}{M_\rho^2 - 4\mu^2} \right)^{3/2}$$
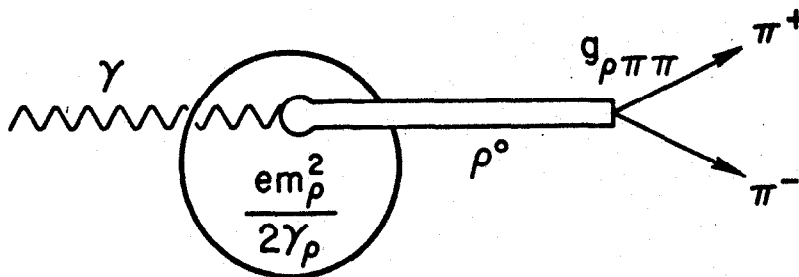
and $C_0, C_1, C_2, M_\rho, \Gamma_\rho$ are free parameters, the last two being the mass and width of the rho. This model assumes that the rho meson production amplitude is given by the Breit-Wigner form, and that it interferes coherently with an imaginary amplitude describing the diffractive $\pi\pi$ scattering. This formalism is due to Söding.[14] We find the measured mass and width of the

rho meson do not vary as a function of the photon energy, k, or the atomic number, A, and the mean values are found to be;

$$M_\rho \sim 765 \pm 10 \text{ MeV}$$

$$\Gamma_\rho \sim 145 \pm 10 \text{ MeV}$$

The differential cross section is then found by integrating overall decay angles, and all masses around the rho. A study of the differential cross section may then be used to find the total rho-nucleon cross section, $\sigma(\rho N)$, and the vector dominance coupling constant, $\gamma_\rho^2/4\pi$.[15] The equations used in this analysis[16] are given below.

1430A45

$$\left.\frac{d\sigma}{dt}\right|_{t_{min}} (\gamma A \to \rho^0 A) = \frac{d\sigma}{dt}(\gamma N \to \rho^0 N)\, f\left(\sigma_{\rho N}, \rho(r), t_{min}\right) \qquad (5)$$

$$\underbrace{\phantom{f\left(\sigma_{\rho N}, \rho(r), t_{min}\right)}}$$
integral over the
volume of the
nucleus

Where

$$t_{min} = \text{minimum 4-momentum transfer} \approx - M_\rho^4/4k^2$$

and

$$f\left(\sigma_{\rho N}, \rho(r), t\right)$$

$$= \left| 2\pi \int_0^\infty \int_{-\infty}^\infty b\, db\, dz\, \underbrace{J_0(q_\perp b)}_{\text{Nuclear Shape}} \underbrace{\rho(b,z)}_{\text{Mass Dependence}} \underbrace{e^{i\sqrt{-t_{min}}\, z - \frac{\sigma_{\rho N}}{2} \int_z^\infty \rho(b,z')dz'}}_{\text{Attenuation of Rho}} \right|^2 \qquad (6)$$

Now the A-dependence of $(d\sigma/dt)\big|_{t_{min}} (\gamma A \to \rho^0 A)$ can be used to determine $\sigma_{\rho N}$.

- 8 -

Further, assuming vector dominance and an imaginary forward amplitude, we can write

$$\frac{d\sigma}{dt}\bigg|_{t_{min}}(\gamma A \to \rho^0 A) = \frac{\alpha}{4}\frac{4\pi}{\gamma_\rho^2}\frac{\sigma_{\rho N}^2}{16\pi}\, f\left(\sigma_{\rho N}, \rho(r), t_{min}\right)$$

Thus, a measurement of the forward rho production cross section, and of $\sigma(\rho N)$, together with knowledge of the nuclear density distribution, $\rho(r)$, allows the determination of the photon-rho coupling constant, $\gamma_\rho^2/4\pi$ (i.e., the relative A-dependence may be used to determine $\sigma(\rho N)$, and then the absolute value of the differential cross sections together with $\sigma(\rho N)$ may be used to determine the coupling constant).

The nuclear density distribution used for these calculations was a Wood-Saxon distribution!

$$\rho(r) = \rho_0 \left\{1 + \exp\left(\frac{r-C}{a}\right)\right\}^{-1} \tag{8}$$

$$C = C_0 A^{1/3} \text{ fermi}$$

$$a = .535 \text{ fermi}$$

where C_0 was taken from electron-nucleus scattering[17] as = 1.08, and from nucleon-nucleus scattering[3] as = 1.18.

The published 9 BeV results of the SLAC experiment[11] were obtained using the above formulation, taking C_0 to be A-independent, and equal to the two values given above. The results are shown in Fig. 5. However, if the nuclear radii suggested by Glauber and Matthiae[18] are used (i.e., ~15% variation in C_0 as a function of A) then the total cross section determined from the SLAC BeV data is $\sigma(\rho N) = (34 \pm 5)$ mb.

At this stage we did not include our hydrogen data for two good reasons — (1) it was not ready, (2) the hydrogen amplitude may include, in principle, contributions other than a purely diffractive amplitude — these contributions come from spin flip amplitudes or from exchange of iso-spin, and have been filtered out in the coherent production using nuclear targets. We have now completed a study of our hydrogen and deuterium data at 9 BeV and see no evidence of substantial spin or iso-spin exchange. We therefore feel free to use this data in our overall fit to the A-dependence.
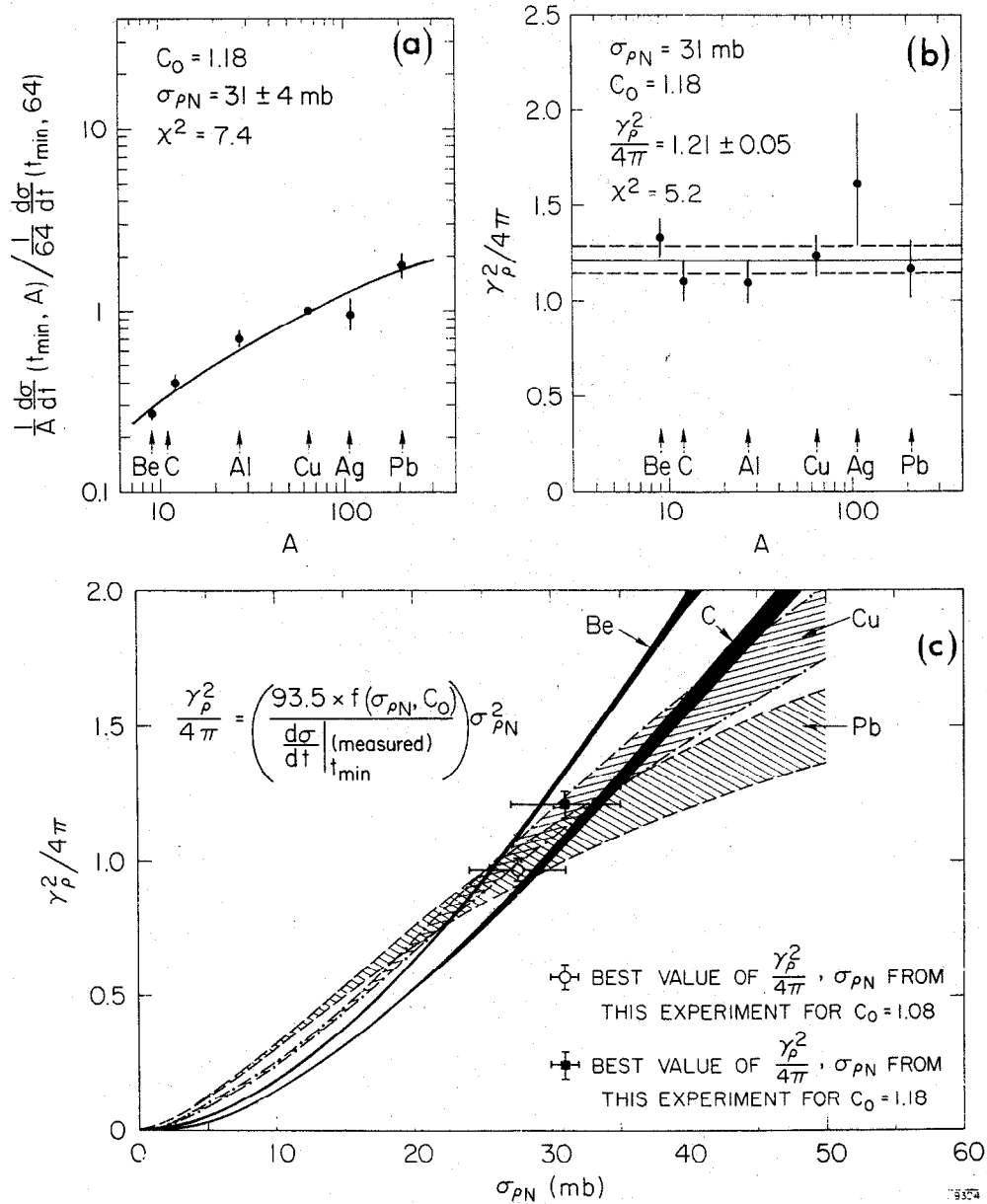
Fig. 5(a)--The forward cross section as a function of A, relative to Cu.
The solid line is the best fit using the optical model described in the text
with $C_0 = 1.18$ fermi; the $\sigma_{\rho N}$ deduced from this fit is (31 ± 4) mb. (Statistical error.) (b) The photon-rho coupling constant as determined from our
forward cross sections and $\sigma_{\rho N}$. The solid line is the best A-independent
fit to the data and gives $\gamma_\rho^2/4\pi = 1.21 \pm 0.05$. (Statistical error.) (c) The dependence of $\gamma_\rho^2/4\pi$ on $\sigma_{\rho N}$ for our measured forward cross sections for
several nuclei. In the relation $\sigma_{\rho N}$ is in barns and $d\sigma/dt$ in mb $(\text{BeV/c})^2$.
The best estimate of $\delta(\rho n)$ and $\gamma_\rho^2/4\pi$ was taken as the mean of the values
obtained with $C_0 = 1.18$ f and 1.08 f.

- 10 -

The mass spectra for the hydrogen and deuterium data is shown in Fig. 6. The solid line represents the best fit using the model described above. The mass and width of the rho are found to be

$$M = 760 \pm 10 \text{ MeV}$$
$$\Gamma = 135 \pm 10 \text{ MeV}$$
Hydrogen, 9 BeV.

$$M = 765 \pm 10$$
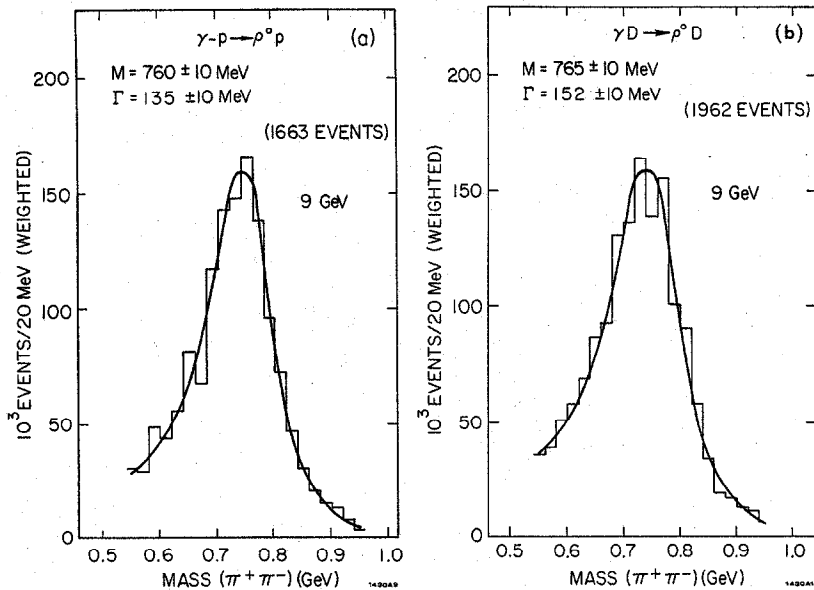$$\Gamma = 152 \pm 10$$
Deuterium, 9 BeV.

Fig. 6--The dipion mass distributions from 9 BeV photon interactions on (a) hydrogen and (b) deuterium. The solid line is the best fit to the data using a coherent mixture of resonant and diffractive background amplitudes.

The decay distribution of rho mesons produced on hydrogen at 9 BeV, is shown in Fig. 7. The solid line is the best fit to the data, using Eq.(3). The density matrix elements are shown in Fig. 8(a) for the helicity system,[19] and Fig. 8(b) evaluated in the Jackson system.[20] We see that the dynamics of the production are such that the rho meson is transversely polarized in the helicity frame, and not in the Jackson system. Density matrix elements from HBC experiments[21] at 4.3 and 5 BeV are shown for comparison. The corresponding data for deuterium is shown in Fig. 9(a) and Fig. 9(b).

The differential cross section for rho production for both hydrogen and deuterium[22] is shown in Fig. 10. The forward cross sections are

found to be:

$$\frac{\gamma\sigma}{\gamma t} (\gamma p \rightarrow \rho^{o} p) = (122 \pm 12) \ \mu b/GeV/c^{2}$$

$$\frac{\gamma\sigma}{\gamma t} (\gamma d \rightarrow \rho^{o} d) = (430 \pm 30) \ \mu b/GeV/c^{2}$$

$$\text{and } R = \frac{d\sigma/dt \ (d)}{d\sigma/dt \ (p)} \bigg|_{t=0} = 3.5 \pm 0.3$$

The value of R expected, after taking into account the Glauber correction, is 3.65, while the Cornell group have measured R, at 6.2 BeV, to be $(3.2 \pm .2)$.[23] Our measurement is in agreement with the expected value of R for the case of pure diffraction, but also agrees, within errors, with the Cornell determination. In addition, we see no differences in the spin-density matrix elements in the forward direction for the hydrogen and deuterium experiments. We therefore conclude that the rho production on hydrogen is dominantly diffractive and use the data in a reanalysis of the A-dependence. When the hydrogen and deuterium data are included in the A-dependence study, the observed effective total rho-nucleon cross section in nuclear matter increases to ~43 mb (see Fig. 11).
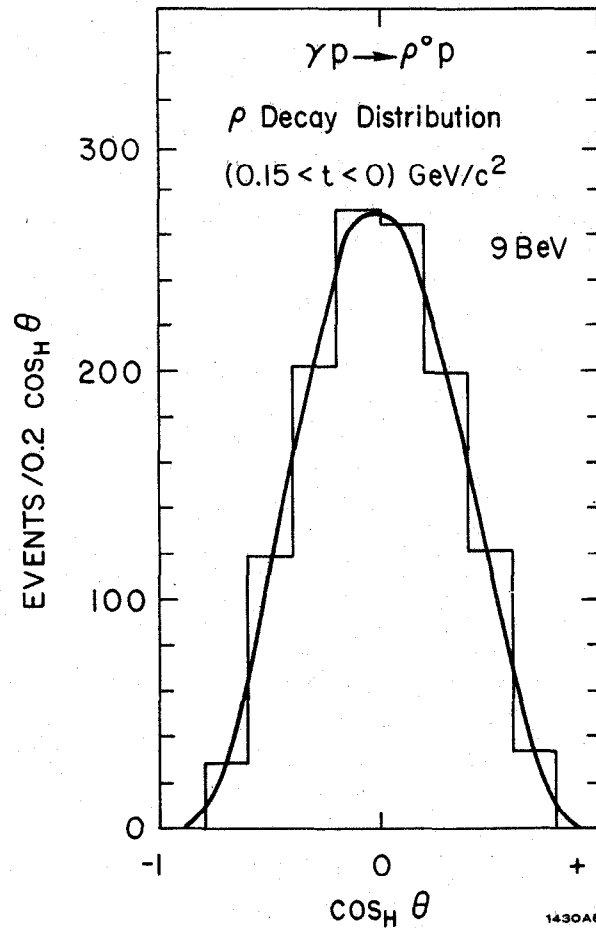

Fig. 7--The observed decay distribution for forward produced rho mesons (i.e., < 0.15 GeV/c^{2}) on hydrogen at 9 BeV. The solid line is a best fit to the data.
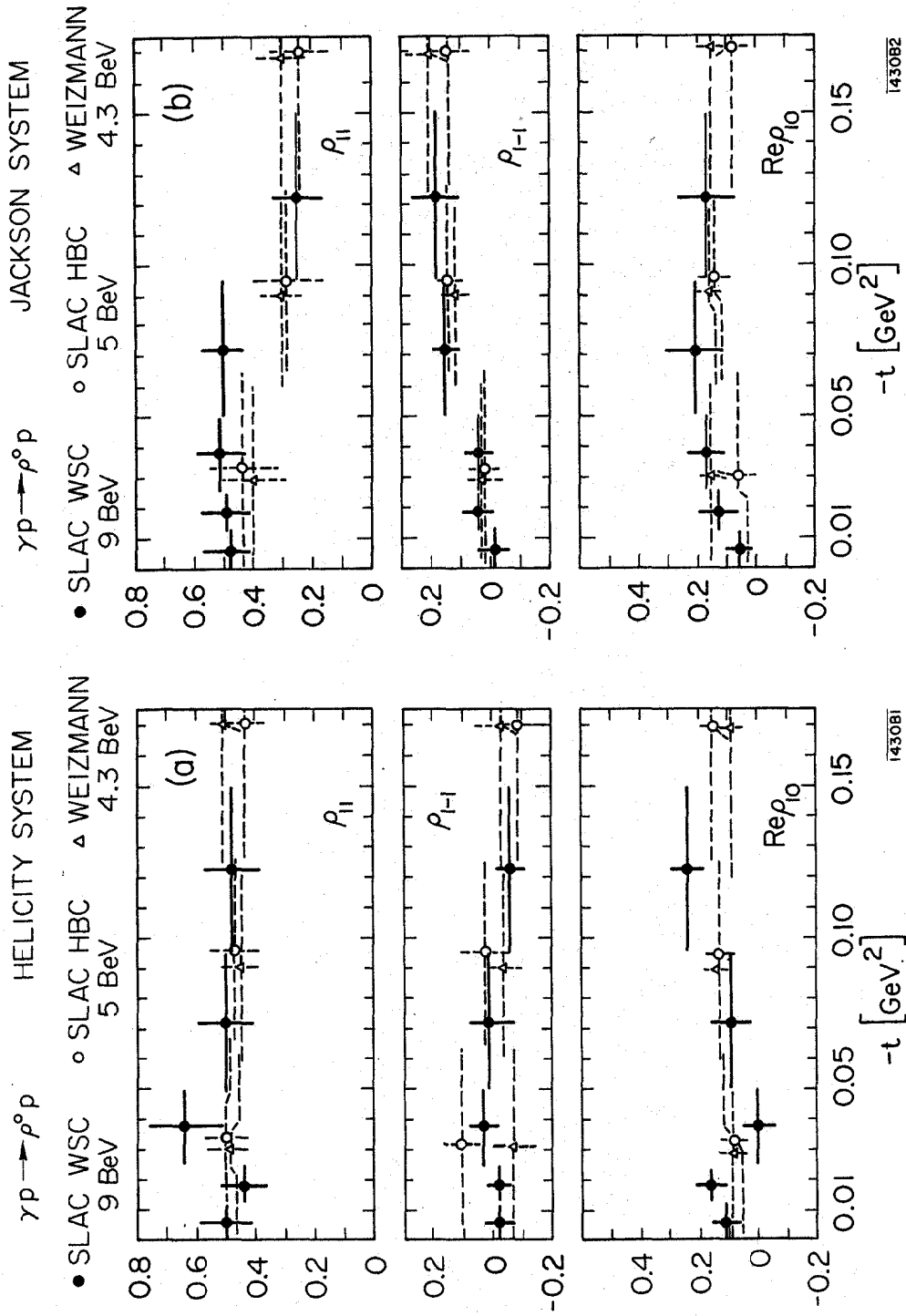
- 12 -

Fig. 8--The spin density matrix elements for rho decay evaluated in (a) helicity frame, and (b) the Jackson frame. The data is from the SLAC wire spark chamber experiment at 9 BeV, the SLAC HBC group at 5 BeV and the Weizmann HBC group at 4.3 BeV.
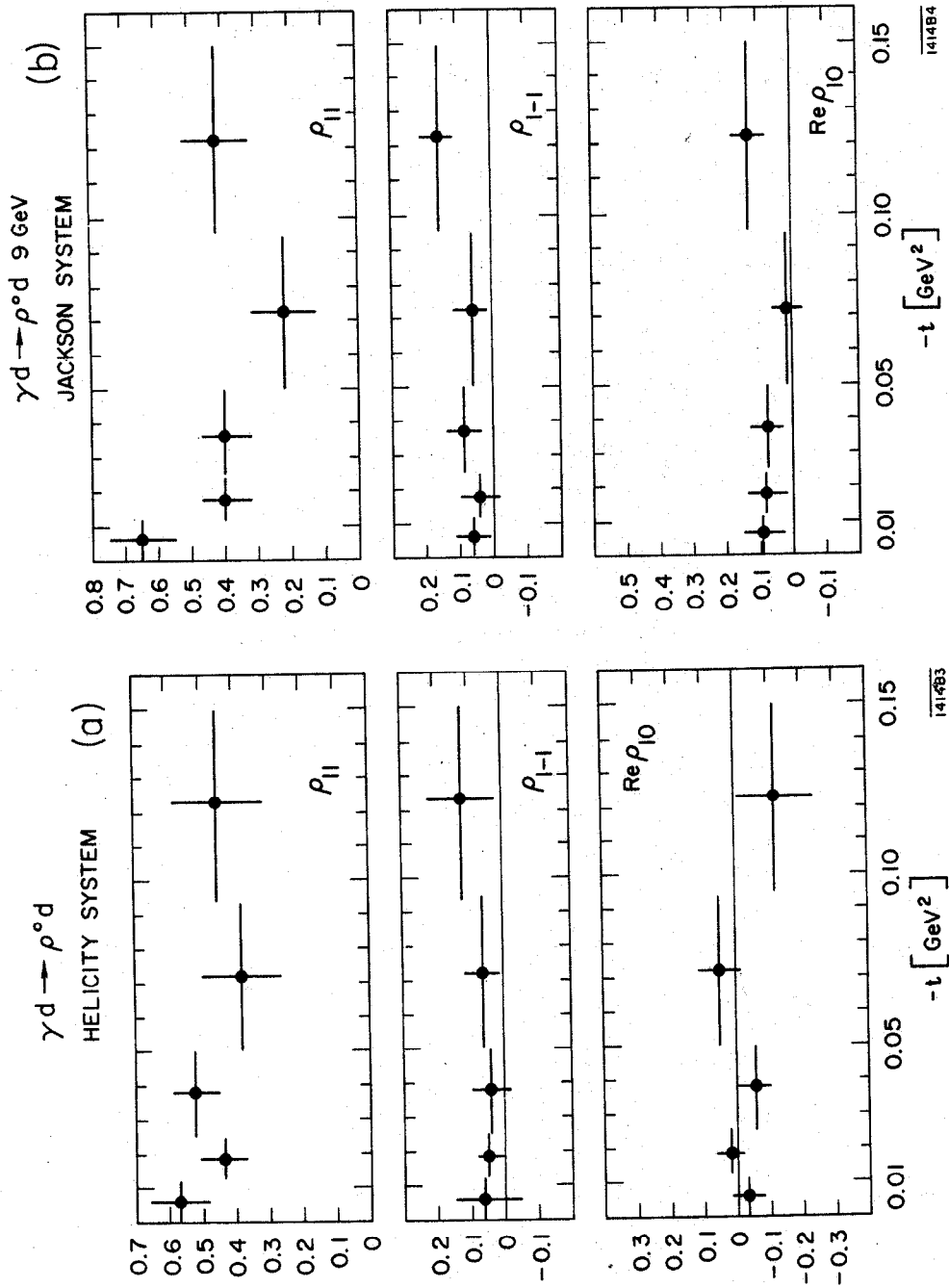
Fig. 9--The spin density matrix elements for rho mesons produced on deuterium at 9 BeV, evaluated in (a) the helicity frame, and (b) the Jackson frame.
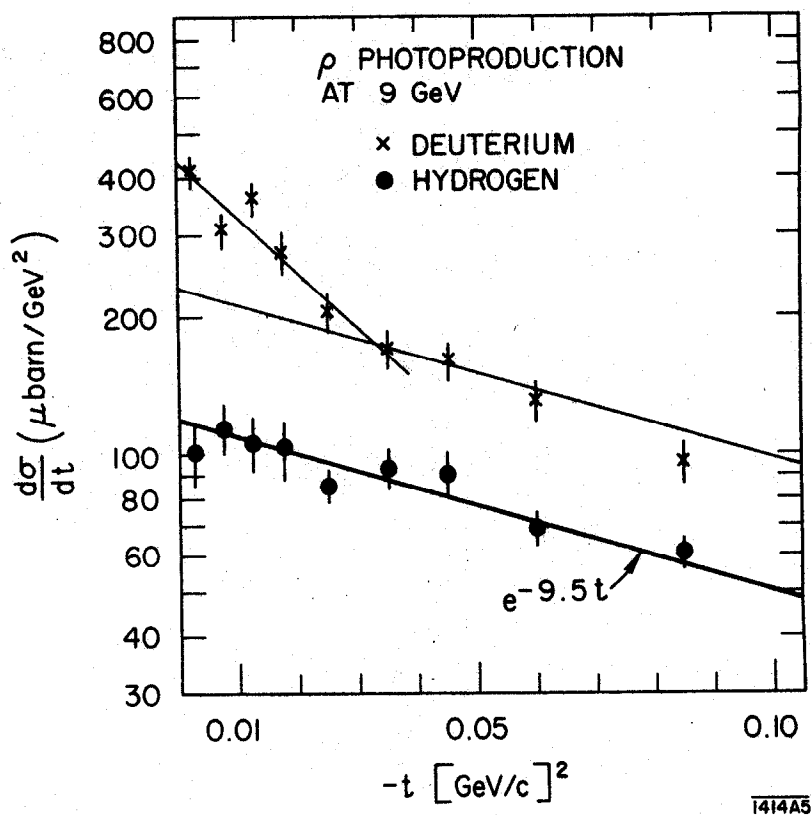
- 14 -

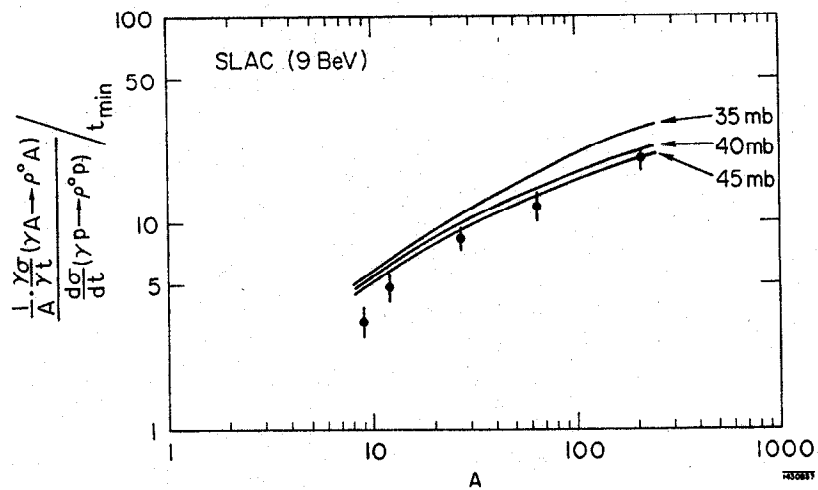Fig. 10--The differential cross section for rho production on hydrogen and deuterium at 9 BeV.

Fig. 11--The A-dependence of the SLAC 9 BeV forward rho cross section.

An alternate method of determining $\sigma(\rho N)$ has been proposed by Silverman,[24] in which the ρ absorption is compared to the observed total cross sections of π's, K's, N's. In Fig. 12 I have plotted the square of the total cross section on nuclear targets, normalized to hydrogen, as a function of atomic number for several incident particles. New data on K_2^0-A total cross sections, presented to this Conference,[25] is included. The solid lines are optical model calculations from Silverman,[24] based on the measured attenuation cross sections of $K^{\pm}, \pi^{\pm}, \bar{p}$, and p on nucleii, at 10.8 and 19 BeV/c, from Galbraith et al.[26]

Also plotted are the ratio, $\partial\sigma/\partial t(\gamma A \rightarrow \rho^0 A)\big/\partial\sigma/\partial t(\gamma p \rightarrow \rho^0 p)$, for the SLAC and Cornell experiments.[9,10] This quantity is related, through VDM, to the ratio $\left[\partial\sigma/\partial t(\rho^0 A \rightarrow \rho^0 A)\big/\partial\sigma/\partial t(\rho^0 p \rightarrow \rho^0 p)\right]$, which in turn is related to $\left[\sigma_T^2(\rho^0 A)/\sigma_T^2(\rho^0 p)\right]$ by the optical theorem. It is clear from the plot that $\sigma(\rho N)$ is more nearly 40 mb than 25 mb.

There is now preliminary data available at 5, 7, and 16 BeV on complex nuclei, from the SLAC group. The forward, and extrapolated differential cross sections are given in Table II. An overall fit to the A-dependence of all the SLAC complex nuclei data yield a total cross section, $\sigma(\rho N)$, ~ 37 mb. If the hydrogen cross section is included in the fit the best estimate of the cross section increases to ~ 42 mb.

Preliminary values of the forward cross section for several targets, as a function of the photon energy, k, is shown in Fig. 13. The solid curve is the prediction of the Drell-Trefil formalism, normalized to the highest energy data points. The measured energy dependence shows good agreement with the model. The extrapolated t=0 differential cross section is shown in Fig. 14 for several targets. The data is certainly in agreement with an energy independent cross section, as would be expected for a diffractive process. However, perhaps more important, the SLAC experiments at different energies (5, 7, 9 and 16 BeV) agree rather well on the k-dependence and A-dependence and seem to represent a self-consistent set of data.

The Cornell group have measured the rho photoproduction cross sections from H_2, D_2, Be, C, Mg, Cu, Ag, Au, and Pb targets at 6.2 BeV photon energy.[10] They use a two-magnet spectrometer with a scintillation counter hodoscope to detect the pions; this setup and their results are described more fully elsewhere.[10,23] Cornell derive $\sigma(\rho N)$ to be (38 ± 4) mb, and $\gamma_\rho^2/4\pi = (1.2 \pm .2)$. It should be noted that they use an A-dependent radius in their analysis (as discussed above), and include the hydrogen cross section in their A-dependence study.

The differential cross sections measured by Cornell are somewhat larger than those published by SLAC. To compare the experiments, I have analyzed the Cornell data using the same phenomenology that has been followed for the SLAC data. The differences are in: (a) the resonance line shape — the SLAC group use a p-wave, energy dependent width for the rho meson, rather than the s-wave, constant width shape of Cornell, (a 7% effect);

- 16 -

(b) the treatment of the background contribution to the dipion effective mass distribution — SLAC fit using a coherent diffractive background while Cornell ignore any background (10-15% effect); (c) the energy dependence of the forward cross section — the forward rho cross section on nuclear targets should show the same energy dependence as the cross section on protons, shown in Fig. 15 (an 11% effect between 6 and 9 BeV). In Table III I have listed the measured Cornell data at 6.2 BeV, the data adjusted (as described above) to show what should be measured at 9 BeV if the Cornell measurements are correct, and finally, the SLAC measured data at 9 BeV. There is clearly good agreement between these experiments.
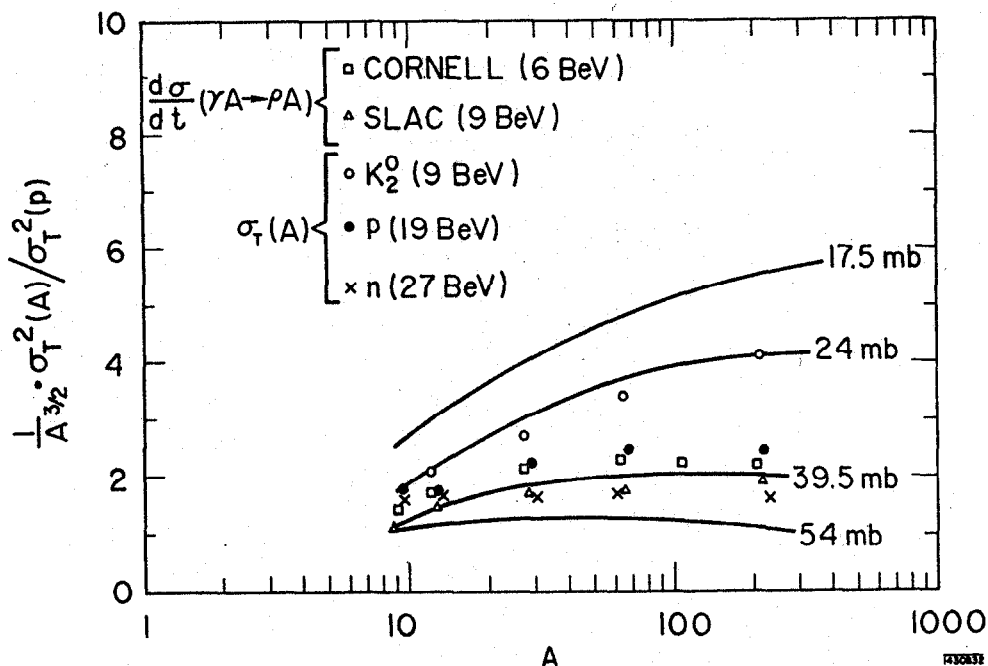

Fig. 12--The A-dependence of the total cross section for K_2^0, p and n compared to rho mesons. The curves are optical model calculations.

TABLE II

SLAC PRELIMINARY DATA ON THE
FORWARD AND EXTRAPOLATED DIFFERENTIAL CROSS SECTIONS FOR $\gamma A \rightarrow \rho^0 A$ (in mb/GeV/c^2)

Photon Energy k (BeV) Atomic Number A	4.83		6.88		8.83		15	
	$\theta = 0^0$	t = 0	$\theta = 0^0$	t = 0	$\theta = 0^0$	t = 0	$\theta = 0$	t = 0
9	$3.49 \begin{matrix}\pm .66 \\ \pm .20\end{matrix}$	$4.40 \begin{matrix}\pm .83 \\ \pm .25\end{matrix}$	$4.21 \begin{matrix}\pm .94 \\ \pm .38\end{matrix}$	$4.72 \begin{matrix}\pm 1.05 \\ \pm .43\end{matrix}$	$3.48 \pm .27$	$3.73 \pm .29$	$4.72 \pm .47$	$4.76 \pm .47$
12	$6.45 \begin{matrix}\pm 1.23 \\ \pm .40\end{matrix}$	$8.31 \begin{matrix}\pm 1.59 \\ \pm .52\end{matrix}$	$8.30 \begin{matrix}\pm 1.83 \\ \pm .70\end{matrix}$	$9.45 \begin{matrix}\pm 2.08 \\ \pm .80\end{matrix}$	$6.85 \pm .74$	$7.39 \pm .80$	-	-
27	$20.0 \begin{matrix}\pm 5.1 \\ \pm 1.7\end{matrix}$	$28.1 \begin{matrix}\pm 7.2 \\ \pm 2.4\end{matrix}$	$33.5 \begin{matrix}\pm 8.2 \\ \pm 3.7\end{matrix}$	$39.7 \begin{matrix}\pm 9.3 \\ \pm 4.4\end{matrix}$	26.7 ± 2.7	29.6 ± 3.0	-	-
64	$72.5 \begin{matrix}\pm 15.2 \\ \pm 5.9\end{matrix}$	$119 \begin{matrix}\pm 25 \\ \pm 10\end{matrix}$	$91 \begin{matrix}\pm 24 \\ \pm 13\end{matrix}$	$116 \begin{matrix}\pm 31 \\ \pm 17\end{matrix}$	90.4 ± 9.2	104.7 ± 10.2	-	-
108	-	-	-	-	147 ± 29	178 ± 35	-	-
208	$268 \begin{matrix}\pm 67 \\ \pm 45\end{matrix}$	$635 \begin{matrix}\pm 159 \\ \pm 107\end{matrix}$	-	-	525 ± 69	677 ± 89	530 ± 67	586 ± 74

k DEPENDENCE OF FORWARD
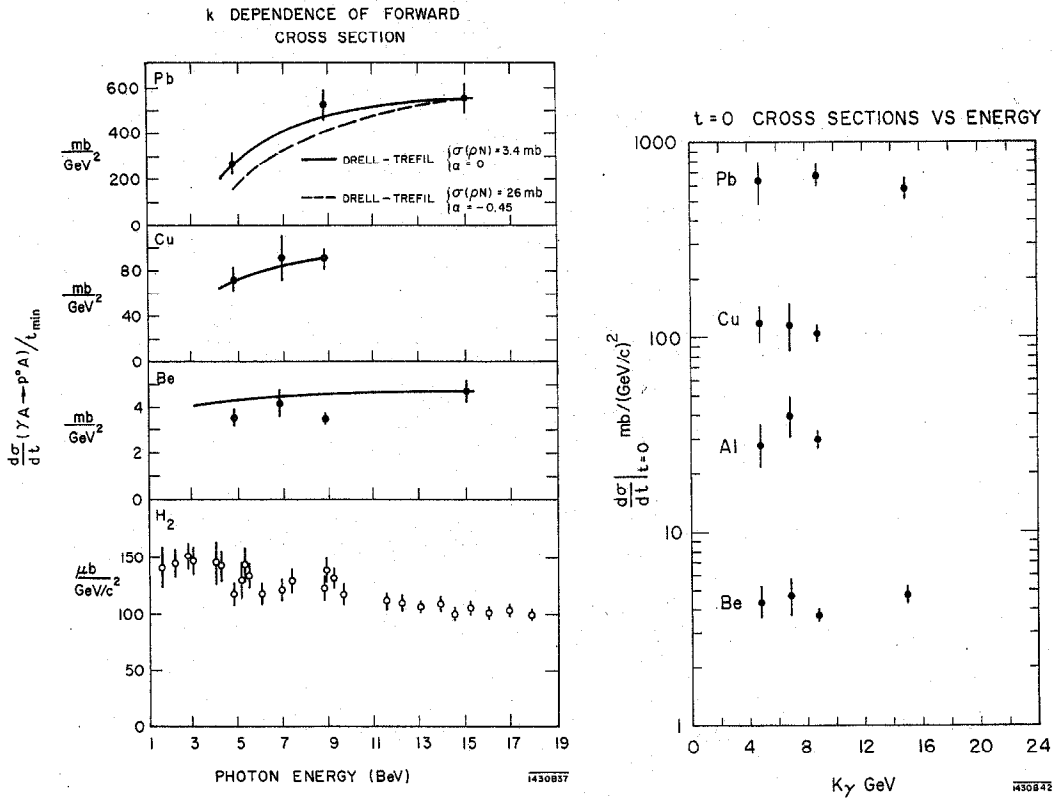CROSS SECTION

t = 0 CROSS SECTIONS VS ENERGY

Fig. 13--The energy dependence of the forward rho cross section for Be, Cu and Pb as measured by the SLAC wire chamber group. The forward hydrogen cross section is shown for comparison.

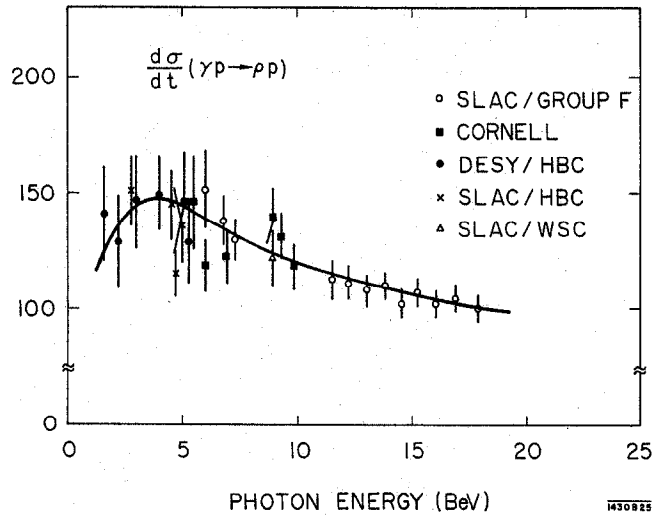Fig. 14--The energy dependence of the extrapolated, t=0, differential cross section for rho production.

Fig. 15--The energy dependence of the forward rho cross section on hydrogen.

TABLE III

CORNELL-SLAC COMPARISON

$$\left[\frac{d\sigma}{dt}(\gamma A \to \rho^0 A)\bigg|_{t=0}\right]$$

Atomic Number A	Cornell Measured Cross Section $(mb/GeV/c^2)$	Cornell Adjusted[†] Cross Section $(mb/GeV/c^2)$	SLAC Measured Cross Section $(mb/GeV/c^2)$
Be	5.4 ± .16	4.01 ± .15	3.7 ± .3
C	9 ± .27	6.7 ± .20	7.4 ± .8
Aℓ	33.3 ± 1.0	24.8 ± 0.7	29.6 ± 3.0
Cu	154 ± 4.5	114.5 ± 3.6	104.7 ± 10.2
Pb	890 ± 26	662 ± 20	677 ± 89

[†]This correction takes into account the different treatment in the mass fitting:
(a) A different Breit-Wigner line shape; (b) Background subtraction. This amounts to 17%. In addition, the k dependence of the $\gamma p \to \rho^0 p$ reaction has been used to compare 6 BeV with 9 BeV. This is an additional correction of 11%.

The third group performing these measurements (DESY/MIT) found results[8] in contradiction to the above experiments. They have now new results from a very beautiful and very systematic experiment which became available only yesterday.[27] They wish to present their data themselves and so Dr. Knasel will present these results himself at the end of this talk. The old experiment did not have data conveniently available for comparison — so very little could be understood of this discrepancy.

We have discussed the new experiment and the data quite extensively and find that the same phenomenology has been followed by both the DESY and SLAC groups, in treating the data (with the exception of evaluating the geometrical efficiency of the respective apparatus), the same features are observed for the background in the dipion mass spectra, the same measured mass and width of the rho and the same measured rho production cross sections on hydrogen. We do, however, seem to differ in our quoted cross sections for nuclear targets.

The results quoted for this new experiment show $\sigma(\rho N) \sim 26$ mb, and $\gamma_\rho^2/4\pi \sim 0.5$ in good agreement with their own previous experiment,[28] but in disagreement with the SLAC and Cornell experiments. The origin of this discrepancy must be found soon, and will only be found by detailed discussion among the three groups involved.

Before leaving this topic, I'd like to discuss briefly two effects which could change the evaluation of the above experiments; — (a) two-body correlations in nuclear matter, and (b) the presence of a large real part in ρ-N scattering.

The existence of two-body correlations in nuclear matter has long been recognized, but the effects have been assumed to be small and the independent particle model of the nucleus has been taken to be adequate.

However, groups at Stanford[29] and McGill[30] have submitted papers to this Conference giving detailed evaluation of this effect on calculations of particle absorption in nuclear matter. The two-body correlation function was evaluated using a "hard-core" repulsive potential together with a short range attractive force determined from the fitting to the low energy nucleon-nucleon scattering data. The two calculations differ in their quantitative conclusions, but both imply $\sim 10\%$ correction for the case of the rho absorption experiments discussed above. This implies that the $\sigma(\rho N)$, deduced from an experiment observing the absorption of rho mesons in nuclear matter should be reduced by $\sim 10\%$ to give the real "free nucleon" cross section.

The effects of a large real part in rho-nucleon scattering have been considered by Talman and Schwartz.[31] They fixed the value of the coupling constant, $\gamma_\rho^2/4\pi$, to the upper limit of the storage ring determination,[32] (i.e., ~ 0.65), and then adjusted the rho-nucleon cross section and α, the ratio of the real to imaginary parts of the ρ-N scattering amplitudes, until they were able to fit the A-dependence of the forward cross section in $\gamma A \to \rho^0 A$. They were able to fit the Cornell data at 6.2 BeV with $\sigma(\rho N)$ ~ 27 mb and $\alpha = -.45$.

I would like to make some observations on the likelihood of such a large real part. The total photon cross section shows an energy dependence very similar to that of the average of $\pi^\pm p$ cross sections. Figure 16 shows the data[33] on $\sigma^T(\gamma p)$, while the solid line is 1/200 of the average of the $\pi^+ p$ and $\pi^- p$ total cross sections. The best fit to the data above 2 BeV is found to be $\sigma^T(\gamma p) = (96.5 + 70/\sqrt{k})\mu b$. Even with this rather arbitrary normalization, the agreement on both magnitude and k-dependence between the photon and hadron cross sections is extraordinarily good. Such an observation would lead one to expect that the real parts involved in the two processes should be comparable; (i.e., $\alpha_{\gamma N} \sim \alpha_{\rho N} \sim \alpha_{\pi^\pm p} \sim -0.2$ at 5 BeV).

Secondly, the total cross section data (extrapolated smoothly to high energies) may be used, with the optical theorem and dispersion relations to evaluate the real part in Compton scattering. This calculation of the dispersion integral has been performed by Damashek and Gilman,[34] and the calculated real part (minus the Thomson term, e^2/m) is shown in Fig. 17. Again this supports a real part in γp (and hence from the vector dominance model in ρN scattering) of $\alpha \lesssim -0.2$ at 5 BeV.

Finally, the inclusion of this large real part only becomes valid if experiments at many energies can be satisfied by approximately the same values of $\sigma(\rho N)$ and α (when allowance is made for their expected smooth, slow energy dependence). The energy dependence of the preliminary SLAC lead and copper data (see Fig. 13) shows disagreement with the predictions of the Cornell parameters. More striking, however, is the A-dependence at high energy. The quantity, $\Delta\sigma(\rho N)/\Delta\alpha$, varies about a factor of ~ 3 between 5 BeV and 16 BeV. The SLAC 16 BeV data could not be made compatible with a $\sigma(\rho N)$ of ~ 26 mb without $|\alpha|$ being > 1.
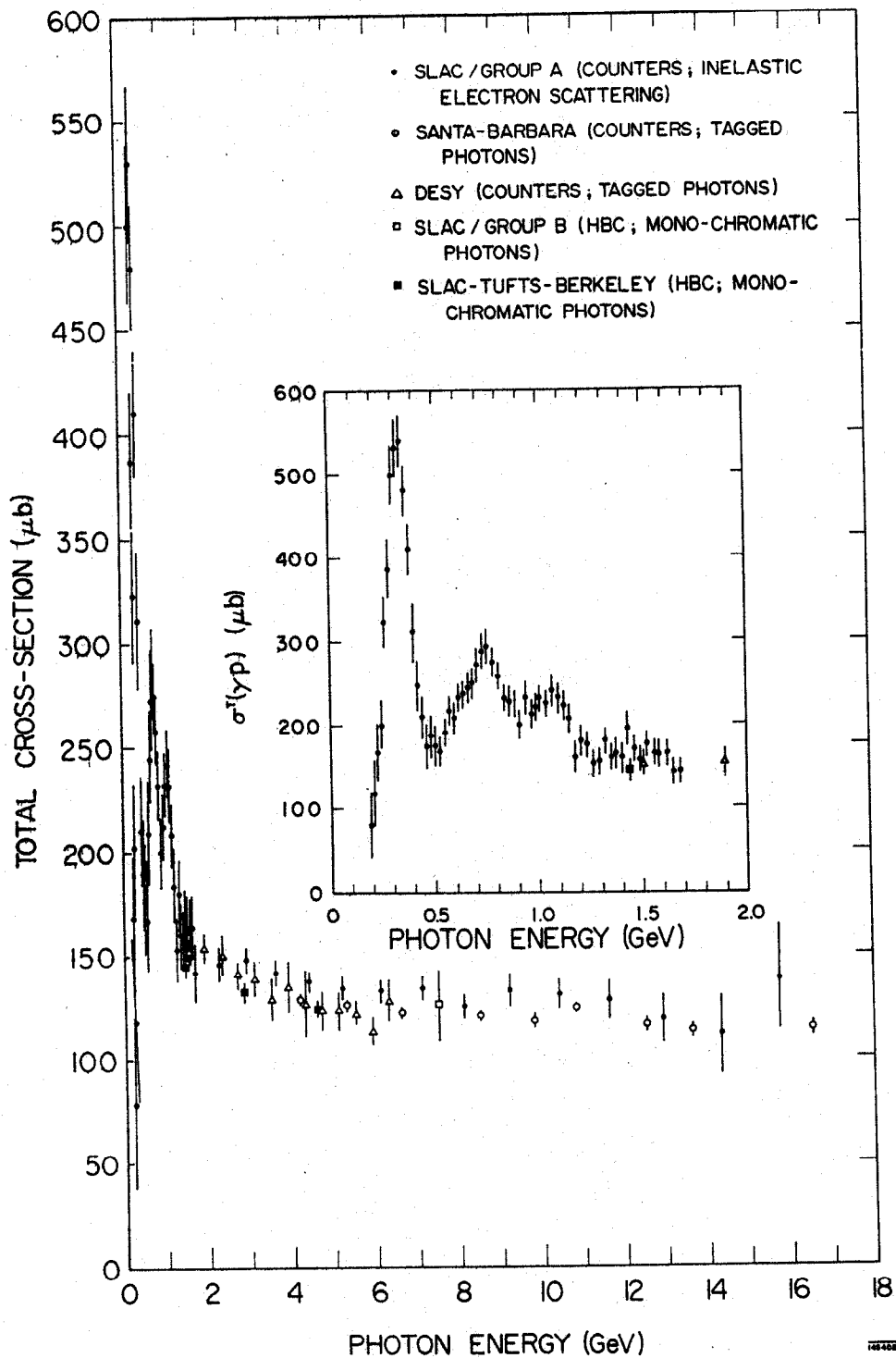
Fig. 16--The energy dependence of the total photon cross section. The solid line is 1/200 of the mean of the $\pi^+ p$ and $\pi^- p$ total cross sections.
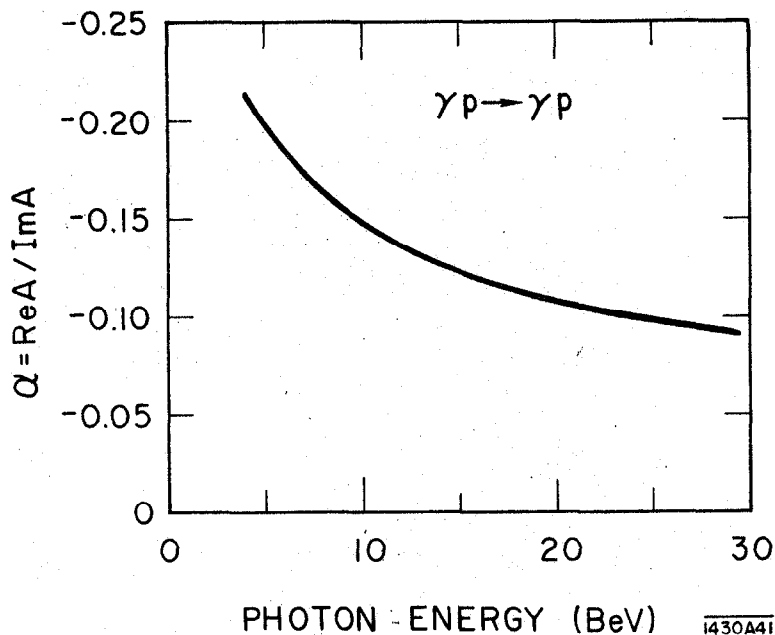
Fig. 17--The ratio of the real to imaginary parts of the Compton scattering amplitude as a function of energy. (The Thomson term, e^2/m, has been subtracted from the calculated value.)

These observations speak against a very large real part, although values $\sim 20\%$ at low energies, decreasing to 10% around 20 BeV, must be expected and included in the analysis of the experiments.

Finally, a summary of the situation in rho photoproduction experiments is given below. I have included the effects of the two-body correlations on the evaluation of $\sigma(\rho N)$.

	SLAC	CORNELL	DESY/MIT
$\sigma(\rho N)$	(35 ± 4) mb	(35 ± 5) mb	(26 ± 2) mb
$\gamma_\rho^2/4\pi$	~ 1.2	~ 1	~ 0.5

III. Total Photoabsorption Cross Sections

Dr. Morrison has just described[35] the elegant experiment performed by the Santa Barbara group at SLAC,[36] measuring the total photon absorption cross sections, in the (8 - 16) BeV region, from hydrogen, deuterium, carbon, copper and lead targets. Similar data is also presented to this conference by DESY[37] in the energy region 1.5 - 6 BeV. I do not intend to describe these experiments, but wish to discuss the results within the framework of vector dominance.

The detailed theoretical calculations for the absorption of photons have been described elsewhere,[38] but may simply be expressed in terms of the following two processes:

1430A47
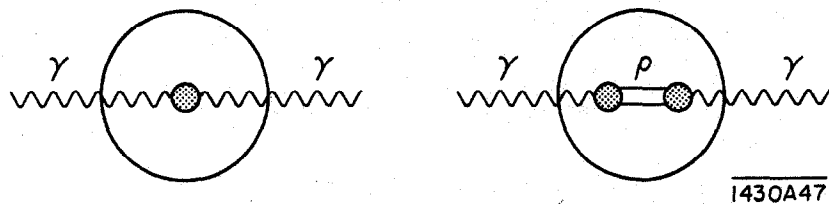
In process (a), the Compton scattering proceeds through the single step of direct interaction with one of the nucleons, whereas in (b) there is an intermediate state of the rho meson — a two-step process. At low energies, the phase difference between these two diagrams is rather large, being given by $\left\{ \exp\left[(m^2_{\pi\pi}/2k)\cdot R \right] \right\}$, and therefore only the left-hand process contributes. This means that the photon is very weakly absorbed and the A-dependence will go as A. At high energies, the phase difference becomes negligible, but the diagrams are 180° out of phase, and so there is complete cancellation. This results in an A-dependence characteristic of the absorption cross section of the strongly interacting particle in the intermediate state of process (b). The A-dependence of the cross section would then be expected to go as the surface area asymptotically, and $\sim A^{0.8}$ at the energies of these experiments. The transition between the 1-step and 2-step domain, or between the cross section varying as A and $A^{0.8}$, is predicted to be in the region 4-8 BeV. The DESY experiment gives the A-dependence as $A^{0.95\pm0.02}$, while UC SB say it is of order $A^{0.9}$. Both experiments yield a value which is neither in one domain nor the other. There is also no observed change in slope as a function of energy. In Fig. 18, we show the energy dependence of the total cross section for several nucleii normalized to hydrogen; the black dots refer to the Santa Barbara experiment while the open circles represent the data from DESY. The consistency between the two experiments is very evident.

The curves show the energy dependence as calculated in the model of Brodsky and Pumplin[38] for various values of the rho-nucleon cross section. The data clearly agree with a cross section of 17 mb or less, and disagree with the 35 mb cross section that would be expected from the SLAC-Cornell determination of $\sigma(\rho N)$. In addition it should be noted that the data do not agree with the 26 mb that is predicted by DESY/MIT experiment.

One comment should be made at this stage on the spectral functions used in the above detailed calculation.[38] The evaluations of the A-dependence of the total photon cross sections have been made using a symmetric, 110 MeV wide mass distribution for the rho, as seen by the storage rings.[32] Now clearly the dipion mass spectrum, as seen in photoproduction, is a very different shape, showing a large shoulder at low $\pi\pi$ masses. These 300-400 MeV dipions will be coherently produced and thereby cause appreciable shadowing, at very low photon momenta.

Therefore, the transition region calculated by these models will in fact be much more gradual than has been presented to date, although at high energies the results will be unchanged.
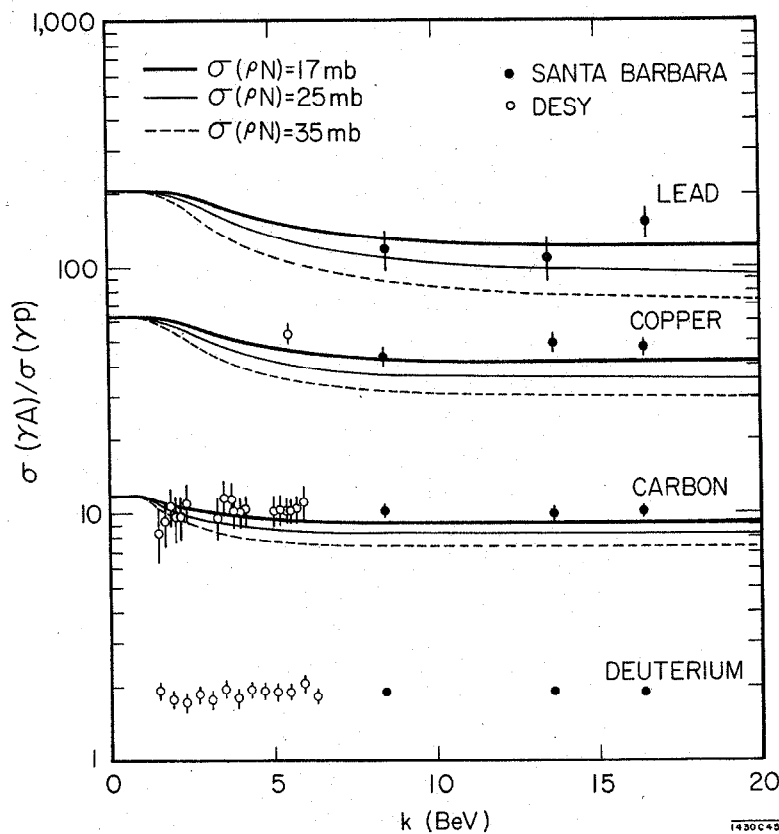

Fig. 18--The energy dependence of the total photon cross section for several nucleii. The curves show the calculated k-dependence for different values of the rho-nucleon total cross section, $\sigma(\rho N)$, using the model of Brodsky and Pumplin with $r_0 = 1.13$ f.

In Fig. 19, the A-dependence of the total cross sections, normalized to hydrogen, is plotted for energies between 5 and 18 BeV. The upper and lower lines reference the case of zero absorption and complete absorption respectively. The total cross section data agree very well between experiments, and for different energies, on a slope just a little less than the zero absorption limit. The other data points on the plot are the square root of the rho photoproduction cross sections normalized to hydrogen, from the SLAC and Cornell experiments. The straight line through these points is the expected A-dependence for a total rho-nucleon cross section of 35 mb.

From the optical theorem and rho dominance[39] it can be shown:

$$\frac{\sigma_T(\gamma A)}{\sigma_T(\gamma p)} = \sqrt{\frac{\frac{d\sigma}{dt}(\gamma A \to \rho^0 A)}{\frac{d\sigma}{dt}(\gamma p \to \rho^0 p)}}\Bigg|_{t=0} \tag{9}$$

This comparison of ratios is independent of nuclear physics and the absolute values of the vector dominance parameters – both sides of the equation can be experimentally measured. The equality of Eq. (9) is badly violated, as clearly shown in Fig. 19, where for lead, the left-hand side is measured as ~140, while the right-hand side gives ~70. This discrepancy has serious implications for vector dominance.

Let us consider, at this stage, a simple model which violates rho dominance, but not the spirit of vector dominance, and which allows a simple description of the above phenomena. First we return to the current field identity:

$$j_\mu^{em}(x) \equiv -\sum \frac{M_V^2}{2\gamma_V} \tag{10}$$

and rather than making the assumption that the rho meson saturates the electromagnetic current, we postulate a series of additional vector mesons of higher and higher masses (or a continuum of p-wave pion pairs) which also couple to the photon. We parameterize this additional contribution as an "equivalent meson," such that:

$$\rho' = \sum V$$

$$M\rho' = \overline{M}_V$$
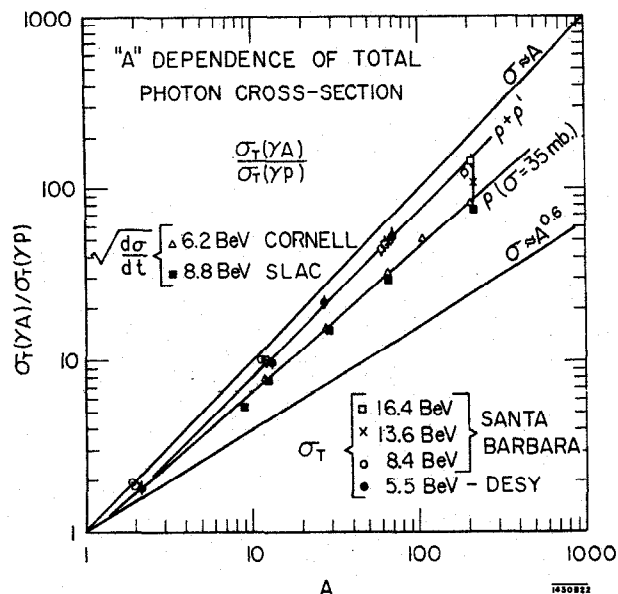
$$\gamma_{\rho'}^2 = \sum \gamma_V^2$$

Fig. 19--The A-dependence of the total photon cross section. Also included is the square root of the t = 0 rho cross sections. These should be equal within the framework of VDM. The upper and lower lines represent the A-dependence expected from zero absorption and asymptotic strong absorption of the photon. The intermediate lines are the predictions of a simple model of photon interactions described in the text.

In this picture the hadronic interaction of the photon is mediated by either the ρ or the ρ' — the relative amounts being given by the coupling constants $\gamma_\rho^2/4\pi$ and $\gamma_{\rho'}^2/4\pi$. The absorption of the photon will depend on the masses of the ρ and ρ' (i.e., only have "strong" absorption when the phase difference $\exp\left[\left(M_V^2/2k\right)\cdot R\right]$ is small), and their total cross sections, $\sigma(\rho N)$ and $\sigma(\rho'N)$.

If the mass of the ρ' is greater than 2 BeV, then at present energies it will not give rise to a coherent amplitude in photoabsorption. This means that the photon absorption will have a contribution which has essentially zero absorption (the ρ' amplitude) and a contribution which has strong absorption (the ρ amplitude). The A-dependence, and the k-dependence of the total photon cross section may be used to determine the relative amounts of the ρ and ρ' amplitudes, and also the minimum mass of the ρ'. Measurement of the coherent rho photoproduction cross section may be used to fix the parameters of the ρ amplitude, since even if $\rho'\to\rho$ coupling is substantial, the ρ' amplitude is not coherent at these energies and does not contribute.

Quantitatively, the coherent rho experiment gives $\sigma(\rho N)\sim 35$ mb, and $\gamma_\rho^2/4\pi\sim 1.2$. The fit to the total cross section data implies the ρ and ρ' amplitudes are equal and that the effective mass of the ρ' be greater than 3000 MeV. Figures 19 and 20 show the A-dependence and k-dependence respectively, as calculated from this model. They are in good agreement with the data.
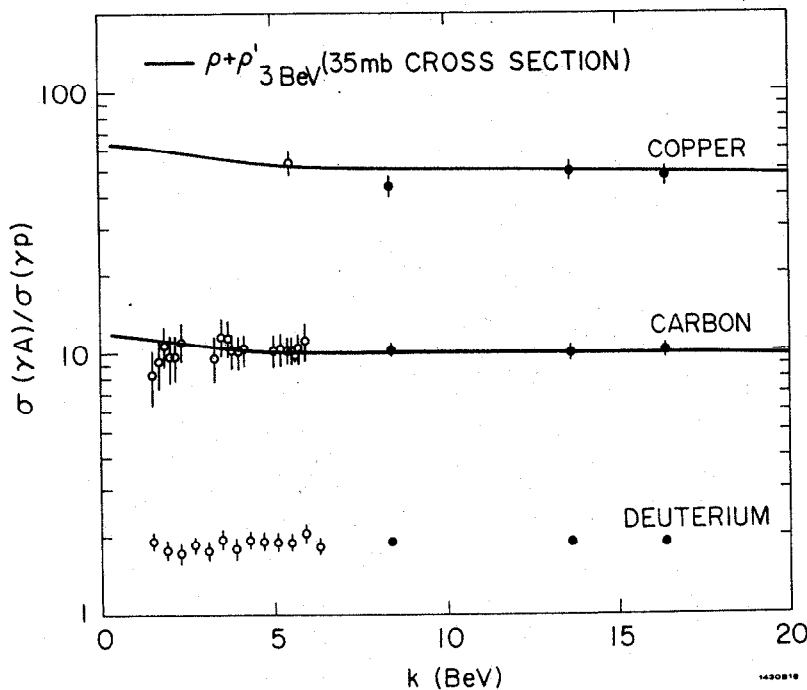

Fig. 20--The A-dependence of the total cross section, with the predictions of the simple model of photon interactions described in the text.

We return now to the discrepancy between Eq. (9) and the measured data, discussed above. The equation should be rewritten as

$$\frac{\sigma^T(\gamma A)}{\sigma^T(\gamma p)} = \frac{\sqrt{\frac{1}{\gamma_\rho^2}\frac{d\sigma}{dt}(\gamma A \to \rho^0 A)} + \sqrt{\frac{1}{\gamma_{\rho'}^2}\frac{d\sigma}{dt}(\gamma A \to \rho' A)}}{\sqrt{\frac{1}{\gamma_\rho^2}\frac{d\sigma}{dt}(\gamma p \to \rho^0 p)} + \sqrt{\frac{1}{\gamma_{\rho'}^2}\frac{d\sigma}{dt}(\gamma p \to \rho' p)}} \tag{11}$$

The RHS of this equation is $70 + 208/1 + 1 = 139$, for the lead case. The denominator has equal contributions from the ρ and ρ' amplitudes as required by the model fits discussed above, while in the numerator the 70 comes from the measured ρ cross section on lead,[10,11] and the 208 is the ρ' amplitude contribution with no absorption or shadowing (i.e., heavy mass ρ' has essentially zero absorption and consequently $\sigma(A) \propto A$). We see, then, that the new form of the equation is satisfied.

To show that this model also works for hydrogen data, consider the relationship (omitting the ρ' amplitude, for the moment),

$$\sigma^T(\gamma p) \propto \sqrt{\frac{1}{\gamma_\rho^2}\frac{d\sigma}{dt}(\gamma p \to \rho^0 p)} + \sqrt{(\text{term for } \omega \text{ and } \phi)} \tag{12}$$

Here the total photon cross section on hydrogen is related to the forward Compton amplitude, by the optical theorem, which in turn is related to the forward vector meson cross sections by VDM. This relationship has been shown to work well for $\gamma_\rho^2/4\pi \sim 0.4$. Within our simple model, we now rewrite this equation as

$$\sigma^T(\gamma p) \propto \sqrt{\frac{1}{\gamma_\rho^2}\frac{d\sigma}{dt}(\gamma p \to \rho p)} + \sqrt{(\text{term for } \omega \text{ and } \phi)} + \sqrt{\frac{1}{\gamma_{\rho'}^2}\frac{d\sigma}{dt}(\gamma p \to \rho' p)} \tag{13}$$

This relationship is also well satisfied for $\gamma_\rho^2/4\pi \sim 1.2$ and equal ρ and ρ' amplitudes.

We have shown that with a simple model which assumes there are contributions to the hadronic interaction of the photon in addition to the ρ meson, that the new data on total photon cross sections can be explained and made compatible with the coherent rho production data. In addition, we have shown that this model is consistent with the hydrogen photoproduction data.

IV. Search for High Mass Vector Mesons

Several groups have searched for evidence of the photoproduction of high mass vector mesons. These experiments fall into two classes — those measuring directly the 2π decay channel with some spectrometer

arrangement,[40,41,42] and those measuring the effect averaged over all decay modes by searching for peaks in a missing-mass experiment.[43]

In performing these searches, it is important to use the highest energy photons possible to avoid problems from phase space inhibition or kinematic effects (like minimum momentum transfer). In Fig. 21, the 2π effective mass spectrum from the SLAC experiment[42] is shown. This is preliminary data from an experiment at 16 BeV, on a Be target, and using the same spectrometer, described in Sect. II above. No strong structure is seen above the rho meson, up to masses of about 2 BeV. The differential cross section for three dipion effective mass regions are shown in Fig. 22 where the diffractive contribution is clearly seen to decrease as the effective mass increases.

The above experiments set limits of the photoproduction cross sections relative to the ρ meson, for possible vector mesons of width ~ 100 MeV and masses ≤ 1800 MeV of $\sim 2. \, 10^{-3}$ in the 2π mode, and $\sim 4. \, 10^{-2}$ for all decays.
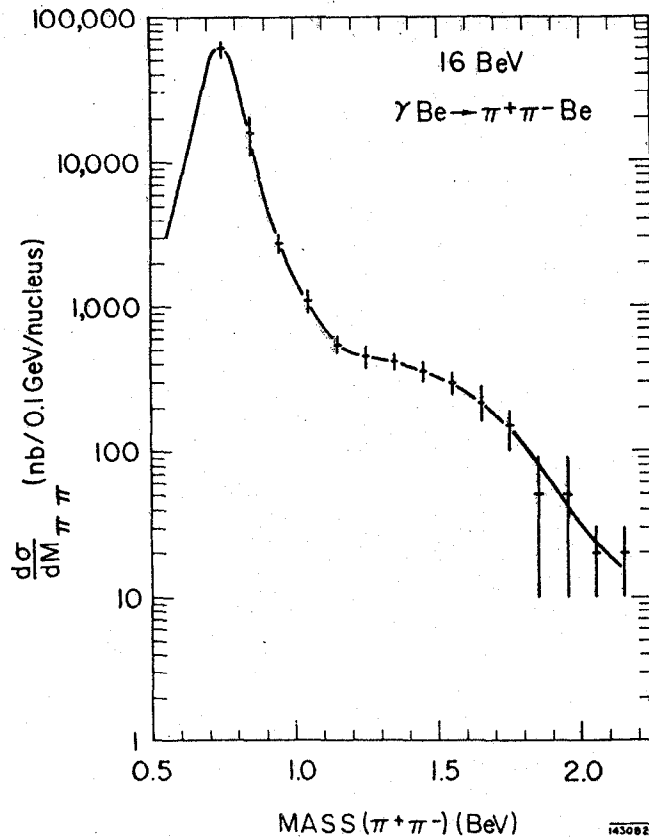

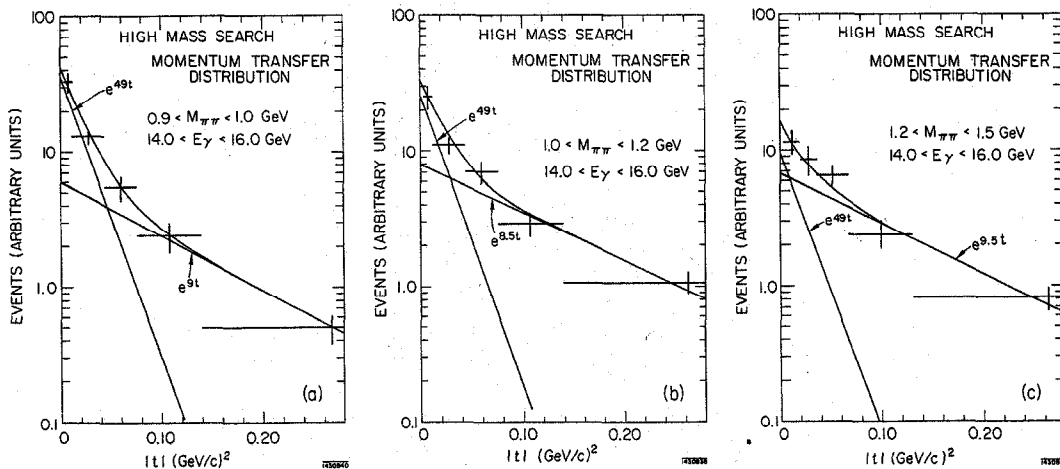Fig. 21--The effective mass distribution for pion pairs produced by 16 BeV photons on a Be target.

Fig. 22--The differential cross section of dipions, produced by 16 BeV photons on a Be target, and with masses of (a) 0.9-1.0 BeV, (b) 1.0-1.2 BeV and (c) 1.2-1.5 BeV.

V. Conclusion

We have reviewed the experimental situation on ρ^o photoproduction and photon absorption in complex nucleii, and shown that there are some disagreements with the VDM. A simple model which extends rho dominance to a generalized vector meson dominance was introduced and was able to take these disagreements into account. We have also shown that for masses up to 1800 MeV, there is no evidence of other vector mesons which couple strongly to 2π and therefore, if this model is correct, the additional contributions to the photon interaction must come from even higher mass states, or from the general continuum of p-wave dipion states.

This leads us to the disagreement between the three experiments measuring coherent ρ^o production. The question remains whether $\sigma(\rho N)$ = 25 mb and $\gamma_\rho^2/4\pi \sim 0.5$, or $\sigma(\rho N) \doteq 35$ mb and $\gamma_\rho^2/4\pi \sim 1.2$ are the correct set of parameters to be drawn from these experiments. The three groups involved have a very real and pressing responsibility to sort out this problem. The situation is upsetting to everybody and can only be sorted out by detailed discussion of the data by the three groups involved. Hopefully this will be done very soon.

In conclusion, I think these experiments using nuclear targets have proven to be very useful tools in understanding high energy physics phenomena. The problems of nuclear models and nuclear physics theory, although present, are indeed much less than have been imagined — for experiments trying to determine elementary particle properties to an accuracy of 10 percent, the understanding of nuclear physics, I am sure, is quite sufficient. Finally, I'm sorry that I can't paint a pretty picture of how everything goes together and how vector dominance works beautifully, but it just doesn't at this stage.